

Accepted Manuscript

Title: Continuous hydrogen production by sorption enhanced steam methane reforming (SE-SMR) in a circulating fluidized bed reactor: Sorbent to catalyst ratio dependencies

Authors: Bjørnar Arstad, Joanna Prostek, Richard Blom



PII: S1385-8947(12)00271-9
DOI: doi:10.1016/j.cej.2012.02.057
Reference: CEJ 9008

To appear in: *Chemical Engineering Journal*

Received date: 18-10-2011
Revised date: 17-2-2012
Accepted date: 20-2-2012

Please cite this article as: B. Arstad, J. Prostek, R. Blom, Continuous hydrogen production by sorption enhanced steam methane reforming (SE-SMR) in a circulating fluidized bed reactor: Sorbent to catalyst ratio dependencies, *Chemical Engineering Journal* (2010), doi:10.1016/j.cej.2012.02.057

This is a PDF file of an unedited manuscript that has been accepted for publication. As a service to our customers we are providing this early version of the manuscript. The manuscript will undergo copyediting, typesetting, and review of the resulting proof before it is published in its final form. Please note that during the production process errors may be discovered which could affect the content, and all legal disclaimers that apply to the journal pertain.

Continuous hydrogen production by sorption enhanced steam methane reforming (SE-SMR) in a circulating fluidized bed reactor: Sorbent to catalyst ratio dependencies

Bjørnar Arstad*, Joanna Prostek, Richard Blom

SINTEF Materials and Chemistry, P.O.Box 124 Blindern, N-0314 Oslo, Norway

e-mail: bjornar.arstad@sintef.no, phone: +4798243498

Abstract

Continuous hydrogen production by sorption enhanced steam methane reforming (SE-SMR) has been studied using a circulating fluidized bed reactor with calcined natural dolomite as CO₂ sorbent and Ni/NiAl₂O₄ as catalyst. A steam to methane ratio of 4 was used at 575 °C and ambient pressure. Two experiments, each run for 8 hours, were carried out using two different volumetric catalyst to sorbent ratios; 20/80 (experiment A) and 50/50 (experiment B) respectively. In experiment A, run at lower than equilibrium conversion, an initial high conversion that dropped significantly after a few hours was observed, while in experiment B, a stable performance throughout the eight hours time-on-stream close to equilibrium conversion of methane was observed. The experiments show that a circulating fluidized bed reactor configuration is suited for SE-SMR for extended time of operation. The sorbent and catalyst materials we have used appear to have quite good mechanical properties at the time scale used (8 hours), but only a fraction of the sorbent's CO₂ capacity appears to be in use.

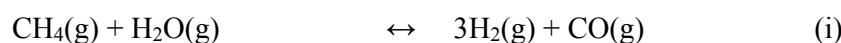
Keywords: sorption enhanced steam methane reforming, circulating fluidized bed reactor, dolomite, hydrogen production

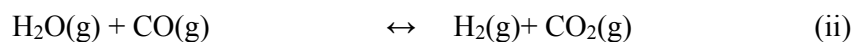
1. Introduction

Schemes for power production from fossil fuels based on hydrogen combustion necessitate decarbonization before energy production (the so-called pre-combustion route). In such technologies either natural gas or solid fuels are transformed into synthesis gas (syngas, H₂ and CO) followed by high and low temperature water-gas shift (WGS) processes to optimize the hydrogen yield. The H₂ and CO₂ are then separated at high partial pressures in a separate step before the power production. State-of-art technologies for CO₂ separation at this point are either processes utilizing physical solvents [1], or pressure swing adsorption (PSA) processes utilizing solid adsorbents [2]. Such processes are commercial in medium sizes, but have still not been demonstrated for full scale power production.

Alternatively to the use of stand-alone processes for CO₂ removal is to incorporate a H₂ or CO₂ separation step in the reforming/gasification/WGS process by the use of membranes or solid sorbents. Major advantages with such approaches are that reactions are driven towards products and that the overall process schemes are simplified [3, 4]. These ideas are not new, and already in 1868 it was suggested to add a solid CO₂ sorbent in a hydrocarbon-steam reforming process [5]. In 1930 the use of calcined dolomite as sorbent when producing hydrogen was patented by Feanz Gulker [6], and in 1933 Williams patented a process where steam and methane react in the presence of a mixture of lime and catalyst to produce hydrogen [7]. In 1963 Gorin and Retallick patented a fluidized-bed process using reforming catalyst together with a CO₂ acceptor [8].

A process applying the principles mentioned above is sorption enhanced steam methane reforming (SE-SMR) [9-11]. In this process steam reforming of methane is carried out catalytically in the presence of a carbon dioxide sorbent (equations i, ii, and iii below). The steam methane reforming (SMR) reaction, eq. (i), and the WGS reaction, eq. (ii), are driven to products by the sorbent's removal of carbon dioxide by carbonate formation, eq. (iii). The total reaction is given in eq. (iv).





MO denotes a metal oxide that is transformed into the carbonate form by its reaction with CO₂. In principle, an efficient carbon dioxide sorbent should be able to pull the reactions fully to the right leading to high yields of hydrogen and negligible concentrations of CO, CO₂, and unconverted methane. Heat integration is quite different in SE-SMR compared to conventional steam reforming. Hydrocarbon reforming is endothermic but by inclusion of a carbonate forming sorbent the total reaction becomes close to being thermo neutral. The exothermicity of the carbonate forming reaction will vary depending on the applied sorbent and by using CaO as the active phase equation (iv) is slightly exothermic at 550-600 °C. However, regeneration of the spent sorbent demands heat and, in the case of CaO based sorbents, the necessary heat is in the range of the heat needed for steam reforming of methane. Hence, the main energy effort in SE-SMR is for the sorbent regeneration step. In spite of the energy demands of the regeneration step simulations have shown that CaO based SE-SMR processes can achieve thermal efficiencies (net efficiencies in parenthesis) as high as 82% (79%) compared to 71% (71%) for a conventional process scheme including amine based CO₂ capture [12].

Previously, we, and others, have demonstrated SE-SMR using a single fluidized bed (FB) reactor in a gas switching mode [13, 14]. However, it has been suggested that a circulating fluidized bed reactor would be particular useful in the SE-SMR process [9, 15] due to continuous cyclic regeneration of the sorbent. In this article we report work that extends significantly our initial demonstration run of SE-SMR in a circulating fluidized bed reactor [16]. In the present work results obtained from two different sorbent/catalyst ratios experiments are presented; one experiment (experiment A) had low methane conversion giving information about deactivation trends, and one experiment (experiment B) had a methane conversion close to thermodynamic equilibrium. Various operational aspects are discussed, including powder attrition.

2. Experimental

2.1 Sorbent preparation: Natural dolomite, $\text{CaMg}(\text{CO}_3)_2$ with about equimolar amounts of Ca and Mg, from the Seljelid field in northern Norway was kindly donated by Hammerfall Dolomitt AS. In order to transform it into a CO_2 acceptor material the dolomite was crushed somewhat and then calcined to a CaOMgO mixed oxide by heat treatment in air at 900 °C followed by 1 hour in 10% H_2 , balanced by N_2 . This material was further crushed and sieved to a 90-200 micro meter (70-170 mesh) fraction.

2.2 Catalyst preparation: A high nickel loading $\text{NiO}:\text{NiAl}_2\text{O}_4$ (60wt.% NiO) catalyst was prepared in a similar manner as described by Ishida et al. [17]: 101,75g (0.271 mole) $\text{Al}(\text{NO}_3)_3 \cdot 9\text{H}_2\text{O}$ (>98.5% from MERCK) and 179,03g (0.616 mole) $\text{Ni}(\text{NO}_3)_2 \cdot 6\text{H}_2\text{O}$ (>98% from FLUKA) were dissolved in 50/50 mixtures of isopropanol and water making two solutions having approximately 0.9 ml solvent pr. g nitrate salt. The two solutions were mixed together and heated to around 230°C under continuous stirring by using a magnetic stirrer. When the viscosity of the solution has reached a state where the magnet is not moving the mixture is transferred to a heat chamber kept at 150°C. The mixture is left in the heat chamber for a couple of days, and then the dry product is transferred to a mortar and crushed. The powder is calcined in air using the following program: 5°/min to 1200°, then kept at 1200°C for 6 hrs. The final powder is then crushed down and sieved. The 70-170 mesh fraction is used in the fluidized bed testing. The synthesized catalyst in oxide form, $\text{NiO}/\text{NiAl}_2\text{O}_4$, was ex-situ reduced in a 10% H_2 atmosphere at 650 °C for 1 hours before applied to the reactor system. We found proper reduction conditions by a temperature programmed reduction in 10% H_2 in Ar from ambient temperature and up to 900 °C (heating ramp 15 °C/min). These data showed that the catalyst was close to fully reduced below 650 °C. In a work by Jin et al. it was observed that $\text{NiO}/\text{NiAl}_2\text{O}_4$ was fully reduced at 600 °C in less than 10 minutes [18].

Predetermined amounts of catalyst and sorbent were mixed together before introduced to the reactor. The total volume of powder that was used in each run was 160 ml. In experiment A the amount sorbent was 32 ml (about 26 g using a bulk density of 0.8

g/cm³) and in experiment B the amount sorbent was 80 ml (about 64 g). Table 1 gives various powder data and related information.

<Table 1>

2.3 Circulating fluidized bed reactor: The reactor system is schematically drawn in Figure 1.

<Figure 1>

The basic configuration, dimensioning, and construction were determined from own experimental results and experience [13], and literature reports on reactor design for SE-SMR [15]. The whole unit is termed the “reactor system” and it includes two different parts/”reactors” where chemical reactions take place, a riser, and two loop seals. In order to better differentiate where reactions take place the parts where the steam reforming and CO₂ sorption take place is termed “the reformer”, and analogously, the part where the sorbent is regenerated is termed “the regenerator”. There are five gas inlets: One each for the reformer and the regenerator, one for each loop seal and one for the riser. The gases enter through porous metal plates (sinters) with an average pore diameter of around 20 μm. All gases leave the reactor system through pipes at the top of the reformer, and the regenerator. The inner diameter of the reformer and regenerator are 5 cm. In both these parts, there is an overflow pipe, which has outer diameter slightly more than 1 cm, and a height of 4 cm. These overflow pipes are placed slightly asymmetric in the reactors and pass through the sinters and wind box, where the inlet gases enter, and down to a connection point with a loop seal. The reactor’s bed heights are fixed at 4 cm and the volume from the sinter to the overflow pipe rim is approximately 75 ml. The two loop seals have a base area of 2*2 cm² and the overflow rim is 4 cm above the sinter. The volume of each loop seal below the overflow rim is around 16 ml. The total volume of powder containing space is thus 182 ml. The volume of the reformer and regenerator each constitutes 41% of the total powder containing volume disregarded the riser. Note that the riser is only used for powder transport - no reaction takes place in this section.

By appropriate pressure balance the loop seals prevents gas mixing between the reformer and the regenerator. The effluent from the reformer is the hydrogen rich stream and consists of nitrogen (used as fluidizing gas in all experiments), hydrogen, CO, CO₂, water, and unconverted methane. The effluent from the regenerator consists of nitrogen and CO₂ liberated from the sorbent with some small amounts of CO.

During operation excess powder flows over the rims and to the next part in the system. Depending on operational conditions and amount of powder a particular powder particle will return to its start after going through all parts of the reactor. The characteristic time for the returning of powder to its initial position is estimated by the powder circulation rate. The powder circulation rate has been estimated in test runs by diverting the riser flow into a measuring vial and the volumetric rate is between 5-15 ml/minute. Direct observation of powder circulation is possible through a glass tube mounted at the riser tube.

At the top of the reactor we have a system for injecting more powder during the runs to compensate for loss of powder due to attrition and other effects, but in the present work no additional powder was added during the runs to make comparisons easier.

A number of thermocouples are used for process control: Each loop seal has its own thermocouple measuring the temperature inside the powder bed about 2 cm above the sinter. The reformer and regenerator each have a thermocouple with four measuring points. These points are located at each centimeter through the powder bed. The temperatures measured in the reformer's bed were relatively uniform with an axial gradient usually around 1 °C but sometimes as high as 2-3 °C. The temperature gradient in the regenerator bed was typically around 5-10 °C. Temperatures were also measured other places in the unit.

During experiments the reformer's temperature were around 570-575 °C and the regenerator's temperature range was mostly around ca. 890-900 °C. These temperature ranges did change during the experiments, typically being most unstable during the first hour of reaction becoming more stable as the experiments progressed. The reformer and regenerator were each located in electrical furnaces for heating the system to operating temperatures and to provide heat for sorbent regeneration. Before

powder circulation commenced the temperatures in the loop seals were around 150-200 °C but increased to 350-550 °C during operation due to hot powder entering from the two reactors. During heating all inlets had a 200 ml/min nitrogen flow. After the temperatures had reached appropriate levels (about 575 °C in the reformer and around 900 °C in the regenerator) the N₂ gas flows were increased to predetermined levels (Table 2). These flow rates have been found in earlier experiments to give adequate operating conditions with the temperatures and powders mixtures we applied.

When the powder started to circulate the temperatures changed significantly in the various parts due to heat transfer and it could take up to one hour to regain the preset operating temperatures of 575 and 900 °C. After thermal stabilization was reached, methane (50 ml/min) and steam (200 ml/min) were added to the 1750 ml/min N₂ flow already applied to the reformer. Table 2 gives flow data during the reforming experiments.

<Table 2>

Total pressure in the system was measured to be 1.0 atm. The pressure difference between the reformer and the regenerator was manually controlled by needle valves. The rig, with its connected lines, is such that during normal operational conditions there is a slightly higher pressure in the reformer compared to the regenerator. This small pressure difference is enough to observe H₂ slippage into the regenerator if no restrictions are put on the regenerator effluent flow. By balancing pressures to avoid H₂ slipping into the regenerator effluent, combined with GC analyses and flow information from the two outlets, we had an operational guideline for balancing the gas flows and pressures in the rig.

At the end of determined experimental times the heating was switched off and all the gas flows were reduced to 200 ml/min N₂. These gas flows were not sufficient to fluidize the powder. Analyses of the used powder from different parts of the unit were therefore possible without too much mixing of powders from one part with another. Note that we do not have the possibility to quench the temperatures so the post-run analyses of the used powders are therefore influenced by the changes in gas composition during cooling.

Cyclones were mounted directly after the two gas outlets to capture particulate matter leaving the reactors due to attrition. In addition, the outlets from these cyclones were directed through water traps to capture fines that had escaped. Water condensation tanks are placed after the water traps before the GC sampling system.

An Agilent micro-GC 3000 was used for gas analyses. Since only one GC was available there are no simultaneous analysis of the effluent gases from the reformer and the regenerator. However, due to the slow variation of gas effluent composition carbon mass balances have been possible to obtain with ok results, *vide infra*.

The dry outlet gas flow rates were measured by Bronkhorst digital mass flow meters. These mass flow meters were calibrated against the mass flow controllers that feed gases into the reactor in order to correct for systematic errors. By combining GC analyses and total outlet flow rates we were able to calculate the dry flow rates of the various gas components in each of the two outlet streams. The flow control system was an in-house custom designed LabVIEW interface.

From measured gas flow rates we have calculated methane conversion, hydrogen yield, and a parameter called “CO₂ separation efficiency”. These are defined below:

The CH₄ conversion is defined as:

$$CH_4 \text{ conversion}/X(CH_4) = \frac{F_{reformer}^{in}(CH_4) - F_{reformer}^{out}(CH_4)}{F_{reformer}^{in}(CH_4)} * 100\%$$

The H₂ yield is defined as:

$$H_2 \text{ yield} = \frac{F_{reformer}^{out}(H_2)}{4 * F_{reformer}^{in}(CH_4)}$$

The "CO₂ separation efficiency" is defined as:

$$CO_2 \text{ separation efficiency} = \frac{F_{regenerator}^{out}(CO_2)}{F_{reformer}^{in}(CH_4) - F_{reformer}^{out}(CH_4)} * 100\%$$

Where the F's denote the flow of the various gases in or out of the regenerator as noted. The H₂ yield is an estimate since it is not corrected for theoretical thermodynamic limits. It is thus slightly underestimated since maximum methane conversion is less than four times inlet flow of methane. The "CO₂ separation efficiency" indicates how much converted methane that leaves the regenerator effluent as CO₂. Due to our single GC we had to pick methane conversion/flow data and CO₂ flow measurements as close as possible in time in order to estimate the CO₂ separation efficiencies. The differences in time between the analyses were about 4-5 minutes. This of course introduces some errors but trends appear to be clear.

Calculation of fluidized bed parameters like e.g. minimum and terminal gas velocities were done using relevant equations given by Kunii and Levenspiel [19] but as we use a mixture of two different powders rigorous estimation of the mixtures properties are difficult. Both our powder types (catalyst and sorbent) are sieved to the same size fraction and the powders are both of Geldart type B. Dolomite has a typical density of 2.84 g/cm³. We may further assume that the density of calcined Dolomite, which we use, is the relative mass fraction remaining after two CO₂ formula units are removed from Dolomite, i.e. ~1.5 g/cm³. Note that the bulk density estimated after light tapping was ~1.0 g/cm³ for calcined dolomite and ~0.8 g/cm³ for the reduced catalyst.

In order to evaluate appropriate gas speeds for fluidization we have estimated various minimum fluidization speeds (U_{mf} , m/s) for a 130 micron large particle with a density 1.5 g/cm³ using the feed gas composition we applied in the reformer using different particle sphericities (ϕ_s) and void fractions (ϵ) at minimum fluidization. The temperature was set to be 575 °C. Since exact data for our powder mixture is quite uncertain we have calculated a range of numbers in order to assess our gas flow rates. These data are given in Table 3.

<Table 3>

Clearly there is a large range of minimum fluidization speeds depending on both the void fraction and the sphericity of the particles. Our superficial gas velocity at the inlet of the reformer, before any conversion with concomitant gas expansion, is about 0.0624 m/s. Based on tabulated values for different solids and conditions compiled by Kunii and Levenspiel it is not unlikely that the voidage in our bed at minimum fluidization is somewhere between 0.5 and 0.6. Since we start with crushed and sieved particles the sphericity is likely somewhat low and might resemble e.g sharp sand ($\phi_s=0.067$) or Fisher-Tropsch catalyst ($\phi_s=0.58$). With these estimates it is likely that the gas speed in our experiments is about 8-10 higher than the minimum fluidization speed. The small temperature gradients in our powder beds also indicate thorough powder mixing/fluidization.

After cooling down overnight in N₂ atmosphere powder samples from different parts of the reactor rig were taken out and a magnet was used to separate the catalyst from the sorbent. After this procedure, the used sorbent samples (four in total, one from the reformer, the regenerator and each loop seal) were transferred to a glove box awaiting further analysis by TGA-MS. We have observed that used sorbent attracts CO₂ and water from air and by storing in a glove box filled with Ar we hoped to minimize absorption from air and make errors systematic and similar for all samples. The TG-MS experiments were carried out by heating the samples in Ar (30 ml/min) from 30 to 900 °C at a rate of 5 °C/min. Water was typically split off in the temperature interval 260-420 °C and CO₂ was liberated in the interval 570-770 °C.

Used sorbent were analyzed using a thermogravimetric analyses connected with a mass spectrometer (TG-MS, NETZSCH STA 449 F1 & QMS 403 C).

Thermodynamic reaction equilibrium values were calculated with Factsage 6.1.

3. Results

After a thermodynamic evaluation of the chemical reaction we present results from the two reactor runs; experiment A and experiment B. The difference between these two runs was the relative amounts of catalyst and sorbent. In the first experiment (exp. A, section 3.2) we used a volumetric ratio of catalyst to sorbent of 20:80 while in the second experiment (exp. B, section 3.3) we used a volumetric ratio of 50:50.

3.1 Thermodynamic simulations

In table 4 we have listed thermodynamic equilibrium data for our reaction system using four different CaO/CH₄ ratios. The initial mixtures for our calculations were: CH₄(g) + 4H₂O(g) + 35N₂(g) + X * CaO(s). X was either 0, 0.5, 1 or 10. The pressure and temperature were set to 1 atm and at 575 °C, respectively.

<Table 4>

As can be seen in Table 4 the methane conversion is high for all cases but the H₂ yield becomes high only at a CaO/CH₄ ratio of 1 or higher. Concomitantly the CO and CO₂ outlet concentrations become low. Note that the CaO/CH₄ ratio of 10 is similar to 1 and is included in order to show data for large ratios. The CO and CO₂ flows have been found from thermodynamic yields of CO/CO₂ * 50ml/min (CH₄ inlet flow rate). In the X=1 run the starting amount of CaO is 1 mole and at equilibrium the calculation gives 0.84 mole CaCO₃. 0.84 * 50 ml/min = 42 ml/min and implies the theoretical maximum CO₂ that can be liberated from the regenerator in our system. It appears that the maximum amount CO₂ that can be delivered to the regenerator is 84 % of the methane feed, and this occurs already at a CaO/CH₄ ratio of 1. Table 4 data can be used to assess if the range of CaO/CH₄ ratio fed to the reformer is higher than or lower than 1, *vide infra*.

3.2 Experiment at low methane conversion (exp A)

This experiment was performed to observe general behavior at less than full methane conversion. Such studies may give information on deactivation and declining performance trends. Gas analyses of the reactors effluent streams were recorded from about 15 minutes after the feed gases were introduced, starting with the reformer. Figure 2 shows the dry gas outlet flow rates from the reformer measured in ml/min.

<Figure 2>

As can be observed there is an initial plateau of about an hour with steady conversion of methane until a decrease take place for the remaining 8 hours. The CO level rises after about an hour to 5 ml/min and then decreases down to about 1.5-2 ml/min after four hours. The CO₂ level is stable around 5 ml/min for the first hour decreasing down to about 3.5 ml/min after 4 hours on stream. Figure 3 displays the methane conversion and H₂ yield. At shutdown the methane conversion was about 5%.

<Figure 3>

Based on calculated thermodynamic data it is clear that experiment A neither reaches the conversion nor the H₂ yield predicted for the reaction even without a sorbent. However, the CO and CO₂ flows from the reformer are much lower compared to the non-enhanced situation, about 2 and 4 ml/min vs. 16 and 33 ml/min for CO and CO₂, respectively, which indicate that there is in fact an enhanced situation.

Figure 4 shows the regenerator effluent concentrations (right axis) and the CO₂ separation efficiency (left axis).

<Figure 4>

The components leaving the regenerator (except for N₂ used as fluidizing agent), were CO₂ with some small amounts of CO (about 0.5 ml/min). Analyses of the regenerator

effluent stream after about 30 minutes to 1.5 hrs. time-on-stream showed a CO₂ flow of about 25-30 ml/min. The observed CO is probably from gas-phase reactions taking place in the freeboard part (i.e. above the powder bed, but before the outlet) of the regenerator. H₂ or other carbon containing gases were not observed in the regenerator effluent stream. There are apparently three regions in the run: One up to 1.5 hours, from 1.5 to 3 hours, and a last period lasting from 3 to 8 hours time-on-stream. In the first period there is a quite stable CO₂ release rate, and in the second period there is a rapid decrease in CO₂ release, while the third period there is a slower (compared to period 2) but steady decrease in CO₂ release. At the start of the experiment the “CO₂ separation efficiency” was around 70-80% decreasing slowly down to around 40%. At the end of the experiment around 50% of the produced CO₂ is found in the reformer effluent. Since the carbonation kinetics and thermodynamic equilibrium are dependent on the partial pressure of CO₂ a low partial pressure result in a small driving force for sorption.

The amount of carbonate in the various parts of the reactor collected after the experiment is shown in Table 5.

<Table 5>

The data shows that small amounts of carbonates are present in all parts of the rig, consistent with the low methane conversion and consequently low CO₂ levels. The results indicate also that there is no accumulation of high density carbonate particles in any part of the rig at the applied conditions. This observation also corresponds with the satisfactory carbon balance.

At shutdown the methane conversion had been low for the last hour with the effects of producing very little CO₂. The TG-MS data therefore correlates well with the GC data. Unconverted steam appears to not adsorb very much in the sorbent at the reaction conditions we applied. In separate TG-MS experiments we have investigated water and CO₂ sorption by a newly prepared sorbent kept in the open in the lab atmosphere. A freshly calcined sample taken with only a short delay from the oven into the TG-MS showed around 2.4 wt.% water and around 1.5 wt.% CO₂. By leaving a batch in air and analyzing samples taken from this batch with one to two days

interval for 9 days we could observe that the water and CO₂ levels stabilized at 16 and 4.5 wt.% respectively after five days. These values are of course influenced by the actual air moisture during these days but the data indicate that there are some remnants of CO₂ even after preparation that is liberated in the TG-MS at high temperature. The 2 wt.% water and CO₂ might be due to a more permanent adsorption as hydroxyl groups and as carbonaceous species on/in the sorbent. With this information in mind it appears that the sorbent analyzed after experiment A did not contain much water nor CO₂ from the SE-SMR reaction.

Powder XRD and BET measurements were carried out on used catalyst powder (catalyst separated from mixture by magnet) but even if some NiO was observed the XRD data did not provide clear indications to what extent the Ni-oxidation had taken place. One point BET indicated a reduction in specific area, about 2.9 to 2.0 m²/g.

The carbon balance in Exp A was usually less than 5% (four measurements had a discrepancy between 6-8 %).

3.3 Experiment at high conversion (exp B)

Experiment B was showed high conversion of methane and Figure 5 shows the dry gas outlet flow rates from the reformer measured in ml/min.

<Figure 5>

Hydrogen dominates the reformer's outlet (except for N₂ which is not shown) with only small amounts of carbon containing gases. Figure 6 shows methane conversion and H₂ yield. There is about 97 (±1) % conversion of methane during the whole run, and the H₂ yield is correspondingly high. The amount of CO and CO₂ leaving the reformer was in average about the same, both around 4 ml/min.

<Figure 6>

When comparing experiment B with Table 4 data it appears that reactions are quite close to predicted thermodynamic values for a system with a CaO/CH₄ ratio higher than 1, except for the methane conversion which is somewhat low, (~97% vs 99.5%).

Figure 7 shows the regenerator effluent composition concentrations (right axis) and the CO₂ separation efficiency (left axis).

<Figure 7>

As in experiment A the main component leaving the regenerator, except for N₂, was CO₂ with some small amounts of CO (around 0.5 ml/min). There is an increase in CO₂ concentration during the first two hours up to a stable performance. Thermodynamic data for CaO/CH₄ ratios of 1 or higher indicates a possible maximum of about 42 ml/min CO₂ released from the regenerator. We observe about 40 ml/min CO₂ leaving the regenerator and we are thus operating close to the maximum thermodynamic CO₂ separation efficiency limit at our applied reaction conditions.

The carbon balance in exp B started out with a discrepancy of 20% in direction of

carbon accumulations inside the reactor. Carbon accumulation is possibly in form of elementary carbon or, more likely, as carbonates. After about 2 hours the carbon balance was good and similar to exp A, around 5-8%. The accumulated carbon gas missing can be estimated to be around 600 ml, i.e. 0.025 moles (0.3g C or 1.1 g CO₂). This amount on the inventory material would constitute about 0.3g/144g inventory material * 100% = 0.21 wt.% accumulated carbon on the powder mixture or it could be about 1.7 wt.% carbonate on the sorbent inventory (64g)

Samples for TG-MS analyses were collected after exp B (Table 5) showed that the main components that were released from the used sorbent upon heating was water and CO₂ as for samples in Exp A.

<Table 6>

4. Discussion

First we will comment on our previous reported work using this reactor for SE-SMR [16]. In reference 16 we demonstrated our reactor unit but the conditions used in that work were later found not to be proper for systematic studies of different powder compositions. The experimental procedures were therefore improved and those applied in the present work were found to give more reliable and consistent data. The differences observed in these two works are likely due to different process conditions and fluid dynamics. In the first paper rather low flow rates were used and another complicating factor was the addition of fresh powder during the run. Before the present work we strived to find conditions that enabled systematic studies when changing the powder mixture.

Between experiment A and B there are quite large differences in methane conversion and H₂ yield. In exp A there is an initial high conversion of methane but after a few hours the conversion falls off drastically, while in exp B the conversion is constant high through the 8 hours. The reason for this difference is likely linked to effects due to variations in the catalyst to sorbent ratio. According to Table 4 the thermodynamic conversion limit in both experiments should be around 98-99% but a conversion close to that is only observed in experiment B. Typically, fluidized bed reactors requires more catalyst than does a fixed bed reactor to achieve a given conversion and the difference in conversion is often rationalized by bubble bypass, bubble emulsion interchange and other mass transfer resistance effects [19]. Our lower observed conversion is thus likely due to flow and transport phenomena we have in our fluidized bed reactor. However, in order to enlighten this issue somewhat we have applied fixed bed kinetic data from Sprung et al.'s work on steam reforming using a similar catalyst as in this work, except with a lower Ni loading, only 2wt.% [20]. At S/C=4, and similar methane partial pressures as we have used (0.022 bar vs. the present work using 0.025 bar CH₄), it is reported a methane conversion rate of about 0.1 molg⁻¹h⁻¹. Their total feed rate was 200 ml/min in an 8 mm inner diameter reactor with about 500 mg of particles out of which 10 mg is catalyst. By assuming a 0.5 ml reactor volume for containment of 500 mg powder the space time can be estimated to be around 0.05s and for methane it is about 0.0013s. This is about a factor of 14

smaller than our space times (see table 2). These estimates indicate that we should have excess catalyst but we observe low conversion in exp A. In Sprung et al. the methane conversion rate for conditions similar to the present work is not changing much over the S/C ratio range of 2 to 4 [20], which implies that the kinetics and mechanisms should not change too much while the gas goes through the fluidized bed. However, in a more realistic reactor operating with e.g. a somewhat lower S/C (2.5 to 3) and no/little extra inert gas the picture changes and there is likely variable conversion rates and governing mechanism through the bed affecting the overall performance. Also relevant to conversion issues is the recent work by Martavaltzi et al. studying various Ni content in hybrid NiO-CaO-Ca₁₂Al₁₄O₃₃ materials [21]. It was found a clear relationship between the active Ni content and conversion in the sorption enhanced system. Up to 16wt.% Ni the conversion levels increased but fell off at 20 wt.% possibly due to an actually lower dispersion of Ni due to large crystallites in the 20wt.% Ni sample. Their observations on the importance of increasing the catalyst amount are in line with our experiments and further support that an optimum ratio of active catalyst components to sorbent components must be found in catalytic sorption enhanced processes either by modeling or by experiments.

The reduction in methane conversion during exp A likely due to some kind of catalyst deactivation. Metal catalyst deactivation is a well know common problem and is often due to sintering(active surface loss) and/or oxidation. In our work Ni oxidation may take place in the reformer by the added steam or in the regenerator due to the release of CO₂ from the used sorbent. Hydrogen produced in the reformer may however counter oxidation by steam. The release of CO from the regenerator may origin from CO₂ oxidizing Ni. In addition the temperature of about 900 °C in the regenerator may induce sintering of catalyst and sorbent. It is out of the scope in this work to investigate in detail deactivation modes of catalyst and sorbent and since our XRD and BET data did not give any clear conclusions on deactivation mode further detailed studies on this topic in SE-SMR must be addressed in other works. It should be noted that Sprung et al observed that their similar catalyst deactivated for the first 120 hours usage [20]. Since catalyst deactivation by nickel surface oxidation is likely a problem a solution may be to add an active component to the catalyst that remains in reduced form during exposure to oxidizing conditions. Deposition of small amounts of noble metal(s) could help keeping the catalyst more active even if the Ni part becomes

oxidized [21]. Another solution could be to introduce H_2 in the regenerator or in the half of the loop seal compartment closest to the riser. With such a configuration no H_2 will enter the regenerator (unused H_2 will go through the riser into the reformer), and if NiO reduction is fast regeneration of oxidized catalyst may take place before it enters the reformer.

From Table 4 thermodynamic CO_2 levels are always significantly higher than the CO level, and in exp A the observed CO_2 levels are about 1.5-2 times larger than CO. In contrast, experiment B show similar amounts of CO and CO_2 , both around 4 ml/min during most of the run. The different trends could indicate change in rates and/or mechanisms through the bed. Han and Harrison reported that calcined dolomite has some shift activity [22], and in exp A we observe more CO_2 than CO. In exp B the CO and CO_2 levels are quite similar hence it might be that the shift activity of the sorbent does not play any important role in this experiment.

Powder attrition is inevitable and in circulating fluidized bed reactors this influence operational aspects quite much. The amounts of fines collected in the cyclones were minimal around 2-4 ml corresponding to less than 3% loss during the eight hours run. However, after a few hours operational time there was observed a reduction in circulation rate most likely due to powder packing effects at various places. Johnsen and Grace did attrition tests in a gas jet attrition apparatus relevant for our work [23], and they measured the attrition of dolomite, limestone and a commercial reforming catalyst at standard ASTM D5757 conditions. They found that after 5 hours operation time there was a loss of 23wt.% dolomite into fines less than 45 μm . We observe significantly less attrition due to lower gas velocities used and possibly also due to the fact that we only use a small fraction of the available sorbent

Consistent with the high methane conversion at the end of exp B the sorbent taken from the reformer has a CO_2 loss of 14.1 wt%. Sorbent taken from the upper loop seal has a CO_2 content of 7.0 wt%. Sorbent samples taken from the regenerator and the lower loop seal both had low CO_2 contents. The difference in CO_2 content in the reformer and upper loop seal can be explained by segregation of heavy carbonate particles in the reformer that will not so easily be circulated in the chosen construction.

It is possible to estimate sorbent circulation rates based on measured CO₂ leaving the regenerator and TG-MS data. In exp A very little CO₂ left the reactor at shut down and therefore data from exp B will be used for the estimation. In exp B the outlet CO₂ flow was about 40 ml/min at shut down, corresponding to 0.00164 mol/min or 0.0719 grams CO₂ leaving pr. minute. TG-MS data show an average of 7.0 wt.% CO₂ in the sorbent taken from the upper loop seal and about 1.9 wt.% CO₂ in the sorbent taken from the regenerator. One may therefore assume that the powder entering the regenerator liberates around 5 wt.% CO₂. 5 wt.% CO₂ of 10 ml sorbent is thus about 0.4 grams or 0.0091 moles CO₂. If released during a minute this amount corresponds to a CO₂ flow of 223 ml/min. Then, a 40 ml/min CO₂ flow originating from a 5 wt.% CO₂ mass loss corresponds to about 1.8 ml sorbent entering the regenerator pr. minute. Since the circulating powder is roughly composed of half sorbent and half catalyst the powder circulation rate becomes around 3.6 ml/min, slightly below the estimates based on diverting the powder flow into a measuring vial. An important point to note is that during all experiment, including those shown here and previous ones, the powder circulation rates are always observed to decrease with time-on-stream. The numbers above are only estimates but they show clearly that for our experiments it is likely that only a fraction of the total CO₂ capacity of the sorbent material is applied.

The powder flow rates can then be used to estimate the fresh sorbent to methane ratio entering the reformer pr. minute during operation. 1.8 ml sorbent corresponds to about 1.4 gram sorbent and when correcting for the MgO part of the material about 0.015 mole CaO units enter the reformer pr. minute. Since 50 ml/min methane is 0.002 moles/min the CaO/CH₄ entering ratio is about 7.5. There are clearly surplus amounts of CaO in both our runs. Our observed CO₂ separation efficiency of about 80% in experiment B thus corresponds quite well with the theoretical limit at the applied conditions.

Sorbent conversion is an important parameter in all sorption enhanced processes and influence reactor size and operational parameters. Likewise, durability and reaction kinetics are also important. Lee has shown that for CaO there is always a rapid sorption interval before a slower sorption process is observed [24]. At 585 °C rapid

sorption is taking place up to about 15% conversion of the CaO. Similarly, Kyaw et al. show that the rapid conversion region for calcined dolomite is up to about 45% conversion at 600 °C, corresponding to about 20 wt.% CO₂ [25]. After the initial fast sorption phase, CO₂ sorption is slow indicating that an outer boundary layer of CaCO₃ is formed and that further sorption becomes bulk diffusion controlled. It appears from estimates above that in our experiments we are clearly operating in the fast kinetic regime. Calcined dolomite can accept about 45 wt.% CO₂, often indicated as 100% conversion, and below is an expression of calcined Dolomite's conversion.

$$\text{Sorbent conversion} = \left(\frac{\left(\frac{m - m_0}{44} \right)}{\left(\frac{m_0}{96} \right)} \right) * 100 = \left(\frac{m_{CO_2}}{m_0} \right) * 100 * 96/44$$

The mass of sorbent with added CO₂ is indicated by m , while m_0 is the initial mass of the CO₂ free sorbent. By working with low sorbent loadings (relatively small m) we are operating mostly in the kinetic regime where the sorption process is fast. In multi cycle experiments using CaO it is observed that the cyclic capacity declines steadily [14, 26, 27]. A main reason for the decline of CaO's sorption capacity has often been reported to be crystallite sintering with the result of increased intraparticle diffusion resistance [see ref 21 and references therein]. By operating in the fast kinetic regime the residence time in the regenerator is short compared to a situation where the full capacity is utilized. In this situation temperature driven deactivations may take place at a later stage (after more hours on stream) due to the relative short exposure to high temperatures. By operating in the kinetic regime and therefore using only a small part of the total sorbent capacity (small m) the makeup flow of sorbent might be much less than if the full capacity is applied. However, such operating conditions results in larger reactor vessels compared to a unit using the full, or close to full, CO₂ sorption capacity as more sorbent mass must be included (large m_0)

5. Conclusion

We have studied SE-SMR in a circulating fluidized bed reactor applying two different powder mixtures, one with 20 vol.% catalyst and another with 50 vol.% catalyst, both balanced by sorbent (80 and 50 vol.% respectively). Each run lasted 8 hours and we used a Ni based catalyst and calcined dolomite as CO₂ sorbent.

Using 20 vol.% catalyst a declining methane conversion was observed with concomitant low H₂ yields, but at the high catalyst loading experiment methane conversion and H₂ yield were high. Using 50% catalyst close to thermodynamic equilibrium conversion of methane and CO₂ separation took place and 97-98% H₂ yield was achieved. A stable performance with respect to gas effluent compositions was observed over the 8 hrs experiment duration. After an initial phase, a steady flow of CO₂ from the regenerator was observed corresponding to 80% CO₂ capture efficiency based on total carbon fed to the reactor. This is close to the thermodynamic separation efficiency in our system at the applied conditions (gas feeds, T_s, pressure).

Comparison with fixed bed kinetic data indicates that conversion levels of methane are drastically lower in our fluidized bed reactor indicating the necessity of using excess catalyst amount relative to a fixed bed situation.

Post run analysis of the used sorbents indicates that only a fraction of the total CO₂ capacity was in use during the experiments. As a consequence circulating fluidized bed reactor designs for SE-SMR (using calcined dolomite) should be aware that only part of the sorbent's capacity could be in use, and combined with the necessary excess catalyst the reactor's size will likely be larger than estimated from fixed bed conversions, and sorbent kinetics and capacities data.

Acknowledgements

The following SINTEF workers are acknowledged for their contribution: Aud I. Spjelkavik for BET, catalyst and sorbent preparation, Anna Lind for XRD data, Jasmina H. Cavka and Anne Andersen for TGA-MS data.

We acknowledge the Research Council of Norway with support through the H2-SER project (grant 178129/S60), and the BIGCCS Centre, performed under the Norwegian research program *Centres for Environment-friendly Energy Research (FME)*. The authors acknowledge the following partners for their contributions: Aker Solutions, ConocoPhillips, Det Norske Veritas, Gassco, Hydro, Shell, Statoil, TOTAL, GDF SUEZ and the Research Council of Norway (193816/S60)

References

- [1] A. Kohl, R. Nielsen, Gas Purification, fifth ed., Gulf Publishing Company, Houston, 1997.
- [2] D.M. Ruthven, S. Farooq, K.S. Knaebel, Pressure Swing Adsorption. VCH, New York, 1994.
- [3] Sorbent enhanced reactions: J. R. Hufton, R. J. Allam, R. Chiang, P. Middleton, E. L. West, V. White, proceedings of the seventh international conference on greenhouse gas technologies, Vancouver (BC), Canada, September 5-9 2004.
- [4] T.A. Peters, M. Stange, H. Klette, R. Bredesen, J. Membr. Sci., 316 (2008) 119-127.
- [5] J.R. Rostrup-Nielsen, in: J.R. Anderson, M. Boudart, (Eds.), Catalysis Science and Technology, Springer, Berlin, 1984
- [6] F. Gulker, Patent GB 301,499 (1930)
- [7] R. Williams, US Patent 1,938,202 (1933)
- [8] E. Gorin, W.B. Retallick, US Patent 3,108,857 (1963)
- [9] D.P. Harrison, Sorption-enhanced hydrogen production: A review, Ind. Eng. Chem. Res., 47 (2008) 6486-6501.
- [10] B.T. Carvil, J.R. Hufton, S. Sircar, Sorption-enhanced reaction process, AIChE J., 42 (1996) 2765-2772.
- [11] L. Barelli, G. Bidini, F. Gallorini, S. Servili, Hydrogen production through sorption-enhanced steam methane reforming and membrane technology: A review, Energy, 33 (2008) 554-570.
- [12] E. Ochoa-Fernández, G. Haugen, T. Zhao, M. Rønning, I. Aartun, B. Børresen, E. Rytter, M. Rønnekleiv, D. Chen, Process design simulation of H₂ production by sorption enhanced steam methane reforming: evaluation of potential CO₂ acceptors, Green, Chem., 9 (2007) 654-662.
- [13] N. Hildenbrand, J. Readman, I.M. Dahl, R. Blom, Sorbent enhanced steam reforming (SESR) of methane using dolomite as internal carbon dioxide absorbent: Limitations due to Ca(OH)₂ formation, Appl. Catal. A, 303 (2006), 131-137.
- [14] K. Johnsen, H.J. Ryu, J.R. Grace, C.J. Lim, Sorption-enhanced steam reforming of methane in a fluidized bed reactor with dolomite as CO₂-acceptor, Chem. Eng. Sci., 61 (2006) 1195-1202.
- [15] K. Johnsen, J.R. Grace, S.S.E.H. Elnashaie, L. Kolbeinsen, D. Eriksen, Modeling of sorption-enhanced steam reforming in a dual fluidized bubbling bed reactor, Ind. Eng. Chem. Res, 45 (2006) 4133-4144.
- [16] B. Arstad, R. Blom, E. Bakken, I. Dahl, J.P. Jakobsen, P. Røkke, Sorption-enhanced methane steam reforming in a circulating fluidized bed reactor system, Energy Proc., 1 (2009) 715-720.
- [17] M. Ishida, M. Yamamoto, T. Ohba, Experimental results of chemical-looping combustion with NiO/NiAl₂O₄ particle circulation at 1200 degrees C, Energy Conv. and Manag., 43 (2002) 1469-1478.
- [18] H. Jin, M. Ishida, Reactivity study on a novel hydrogen fueled chemical-looping combustion, Int. J. Hydrogen Energy, 26 (2001) 889-894.
- [19] D. Kunii and O. Levenspiel, Fluidization Engineering, second ed., Butterworth-Heinemann, Newton, 1991.
- [20] C. Sprung, B. Arstad, U.Olsbye, Methane Steam Reforming Over Ni/NiAlO₄ Catalyst: The effect of Steam-toMethane Ratio, Top. Catal., 54 (2011) 1063-

1069

- [21] C.S. Martavaltzi, A.A. Lemonidou, Hydrogen production via sorption enhanced reforming of methane: Development of a novel hybrid material-reforming catalyst and CO₂ sorbent, *Chem. Eng. Sci.*, 65 (2010) 4134-4140
- [21] L.P.R. Profeti, E.A. Ticianelli, E.M. Assaf, Co/Al₂O₃ catalysts promoted with noble metals for production of hydrogen by methane steam reforming, *Fuel*, 87 (2008) 2076-2081.
- [22] C. Han, D.P. Harrison, Simultaneous shift reaction and carbon dioxide separation for the direct production of hydrogen, *Chem. Eng. Sci.*, 49 (1994) 5875-5883
- [23] K. Johnsen, J.R. Grace, High-temperature attrition of sorbents and a catalyst for sorption-enhanced steam methane reforming in a fluidized bed environment, *Powder Tech.*, 173 (2007) 200-202.
- [24] D.K. Lee, An apparent kinetic model for the carbonation of calcium oxide by Carbon dioxide, *Chem. Eng. J.*, 100 (2004) 71-77.
- [25] K. Kyaw, M. Kanamori, H. Matsuda, M. Hasatani, Study of carbonation reactions of Ca-Mg oxides for high temperature energy storage and heat transformation, *J. Chem. Eng. Jap.*, 29 (1996) 112-118.
- [26] J.C. Abanades, The maximum capture efficiency of CO₂ using a carbonation/calcination cycle of CaO/CaCO₃, *Chem. Eng. J.*, 90, (2002) 303-306.
- [27] B. Feng, W. Liu, X. Li, H. An, Overcoming the problem of loss-in-capacity of calcium oxide in CO₂ capture, *Energy&Fuels*, 20 (2006) 2417-2420.

Table 1. Powder data

	<i>Common values</i>	<i>Exp A</i>	<i>Exp B</i>
wt% CaO in sorbent/mole CaO	57.0*/1.02		
wt% MgO in sorbent/mole MgO	38.6*/0.96		
Molar ratio CaO/MgO	1.06		
Particle size fraction	90-200 μ m		
Bulk density sorbent	0.83 g/ml		
Bulk density catalyst	1.04 g/ml		
Geldart type (Cat/Sorb)	B/B		
Total solid inventory		160 ml/166g	160 ml/149g
Total amount catalyst		32 ml/33g	80 ml/83g
Total amount sorbent		128 ml/133g	80 ml/66g
Estimated amount catalyst in reformer		13ml/14g	33ml/34g
Estimated amount sorbent in reformer		52ml/44g	33ml/27g

*) The remaining mass is various oxides in small amounts.

Table 2. Feed gas flows, and space time values in the experiments.

<i>Unit:</i>	<i>Gas flow rates, ml/min</i>	<i>Superficial gas speed, cm/s ^{a)}</i>	<i>Space time, s ^{a)}</i>	<i>Adjusted space time, s ^{b)}</i>
Reformer	1750 N ₂	6.2 (mix)	0.72 (mix)	0.43 (mix)
	50 CH ₄ (P _{CH₄} =0.025)	0.16	0.018 (CH ₄)	0.011 (CH ₄)
	200 Steam (P _{H₂O} =0.1)	0.62	0.072 (H ₂ O)	0.043 (H ₂ O)
Regenerator	1300 N ₂	5.6	0.81	
Loop seals	450 N ₂			
Riser	1750 N ₂			

^{a)} Superficial gas speeds and space time are based on entrance conditions. The flow rates used are corrected for thermal expansion from room temperature to 575°C(reformer) and 900°C(regenerator).

^{b)} Adjusted space time assumes a bed with a voidage of 0.6, i.e. a "reactor volume" of 45 ml instead of the empty volume of 75 ml.

Table 3. Minimum fluidization speeds (U_{mf} , m/s) at various void fractions at minimum fluidization (ϵ_{mf}) and particle sphericities (ϕ_s) for a 130 micron size particle with a density of 1500 kg/m^3 at $575 \text{ }^\circ\text{C}$ using our feed gas composition (50 ml/min CH_4 + 200 ml/min steam + 1750 ml/min N_2). The average gas density and viscosity for this mixture at $575 \text{ }^\circ\text{C}$ is 0.40 kg/m^3 and $0.000037 \text{ kg/m}\cdot\text{s}$ respectively.

U_{mf}	$\phi_s=0.6$	$\phi_s=0.7$	$\phi_s=0.8$	$\phi_s=0.9$
ϵ				
0.40	0.0017	0.0023	0.0031	0.0039
0.45	0.0027	0.0036	0.0047	0.0060
0.50	0.0040	0.0055	0.0072	0.0091
0.55	0.0060	0.0081	0.0106	0.0134
0.60	0.0087	0.0119	0.0155	0.0196

Table 4. Thermodynamic equilibrium data on CH₄ conversion, H₂ yield, CO and CO₂ flows at 575 °C with the applied gas composition (including N₂) to the reformer as shown in Table 2, and with varying CaO/CH₄ ratio. The CO and CO₂ flows have been found from the yields of CO/CO₂ * 50ml/min.

<i>CaO/CH₄</i> <i>ratio</i>	<i>CH₄</i> <i>conversion, %</i>	<i>H₂ yield</i>	<i>CO flow</i> <i>[ml/min]</i>	<i>CO₂ flow</i> <i>[ml/min]</i>	<i>CaO</i>	<i>CaCO₃</i>
0	98.2	0.90	16.1	33.0	NA	NA
0.5	98.8	0.95	8.6	15.8	0.0	0.5
1	99.5	0.98	2.9	4.8	0.16	0.84
10	99.5	0.98	2.9	4.8	9.16	0.84

Table 5. TGA-MS data from experiment A (weight %).

<i>Experiment A</i>	<i>Water</i>	<i>CO₂</i>
Reformer	1.7	1.8
Upper loop seal	1.7	1.4
Regenerator	1.6	1.3
Lower loop seal	2.0	1.8

Table 6. TGA-MS data from experiment B (weight %).

<i>Experiment B</i>	<i>Water</i>	<i>CO₂</i>
Reformer	3.8	14.1
Upper loop seal	1.4	7.0
Regenerator	1.6	1.9
Lower loop seal	1.8	1.4

Accepted Manuscript

Highlights

- Hydrogen production by SE-SMR in a circulating fluidized bed reactor.
- Hydrogen yields around 0.96 and CO₂ separation efficiencies around 80%.
- Data indicate important aspects related to powder mixture compositions.

Accepted Manuscript

Figure 1: Schematic drawing of the reactor system.

Figure 2: Reformer outlet gas composition (dry basis) in experiment A. The inset shows the CO and CO₂ flows. Feed: 50 ml/min CH₄ and 200 ml/min steam. Catalyst to sorbent ratio: 20:80. T(reformer): 575 °C, T(regenerator): 890-900 °C.

Figure 3: Methane conversion and hydrogen yield in experiment A. Feed: 50 ml/min CH₄ and 200 ml/min steam. Catalyst to sorbent ratio: 20:80. T(reformer): 575 °C, T(regenerator): 890-900 °C.

Figure 4: Regenerator dry outlet composition (right axis) and CO₂ separation efficiency (left axis) based on converted methane in experiment A. Feed: 50 ml/min CH₄ and 200 ml/min steam. Catalyst to sorbent ratio: 20:80. T(reformer): 575 °C, T(regenerator): 890-900 °C.

Figure 5: Reformer dry outlet gas composition in experiment B. The inset shows the CO and CO₂ flows. Feed: 50 ml/min CH₄ and 200 ml/min steam. Catalyst to sorbent ratio: 50:50. T(reformer): 575 °C, T(regenerator): 890-900 °C.

Figure 6: Methane conversion and hydrogen yield in experiment B. Feed: 50 ml/min CH₄ and 200 ml/min steam. Catalyst to sorbent ratio: 50:50. T(reformer): 575 °C, T(regenerator): 890-900 °C.

Figure 7: Regenerator dry outlet composition (right axis) and CO₂ separation efficiency (left axis) based on converted methane in experiment B. Feed: 50 ml/min CH₄ and 200 ml/min steam. Catalyst to sorbent ratio: 50:50. T(reformer): 575 °C, T(regenerator): 890-900 °C.

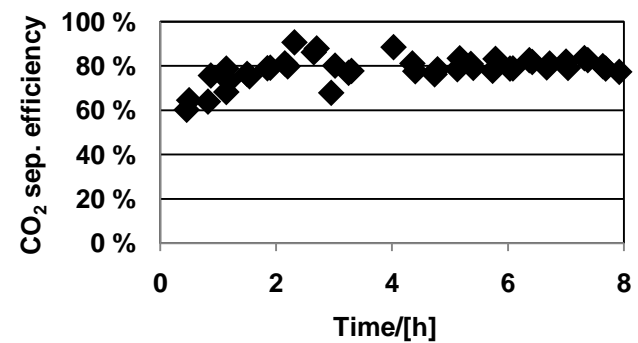
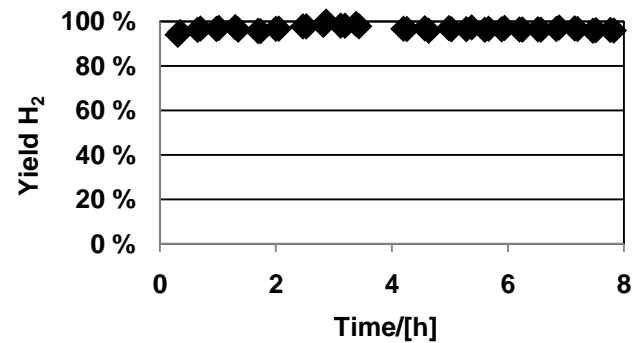
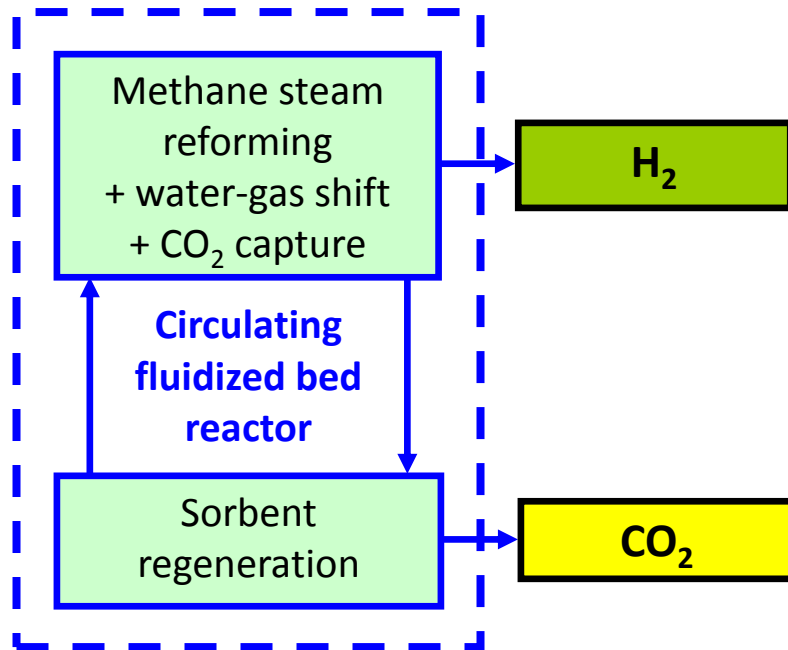


Figure 1

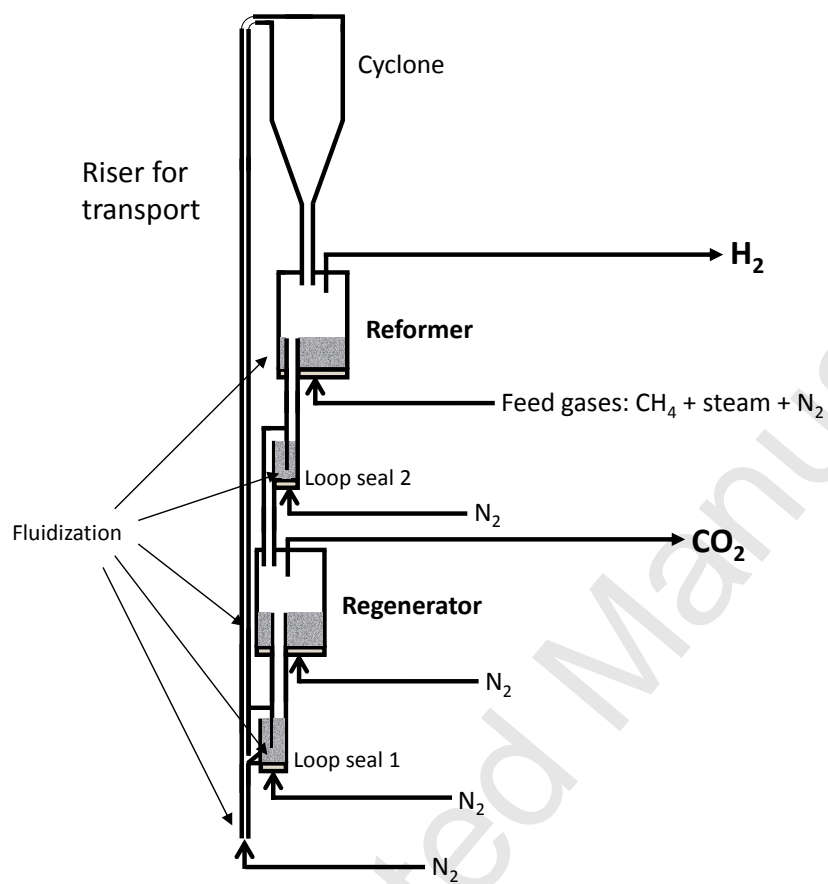


Figure 2

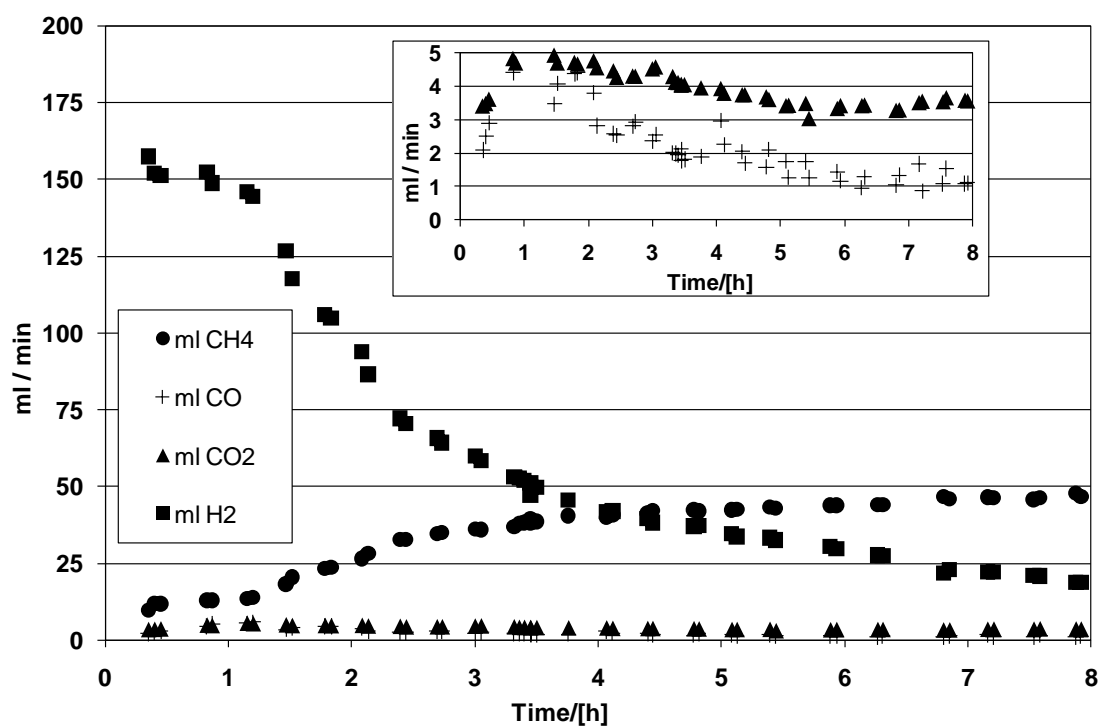


Figure 3

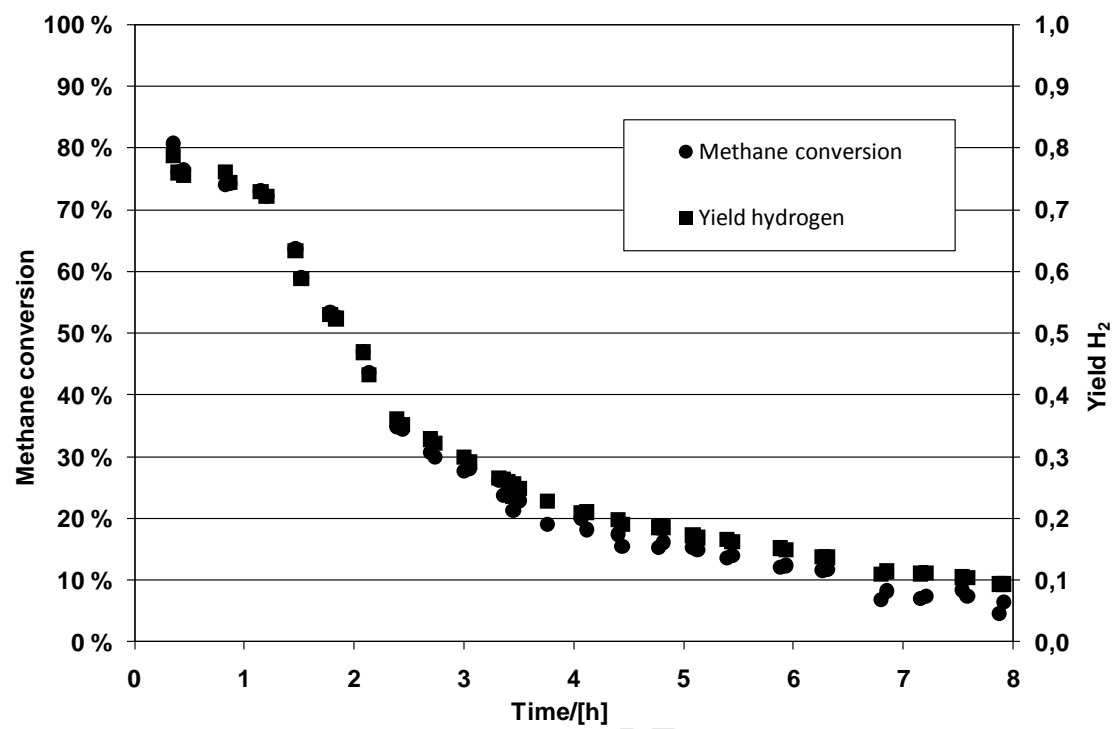


Figure 4

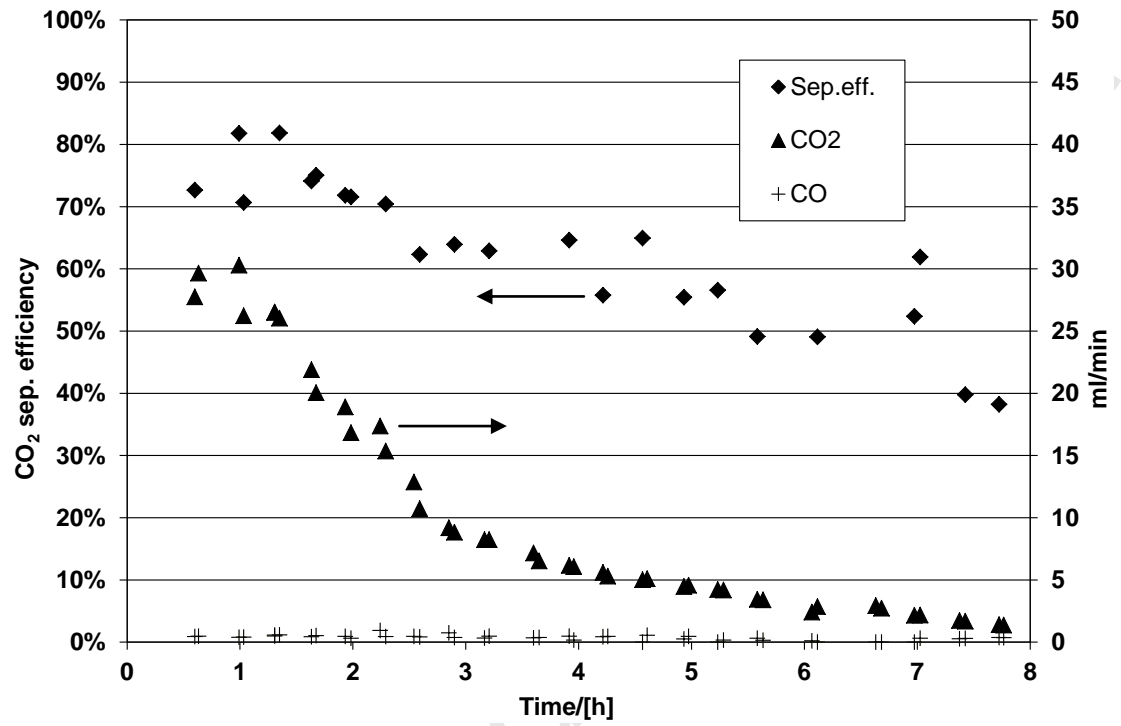


Figure 5

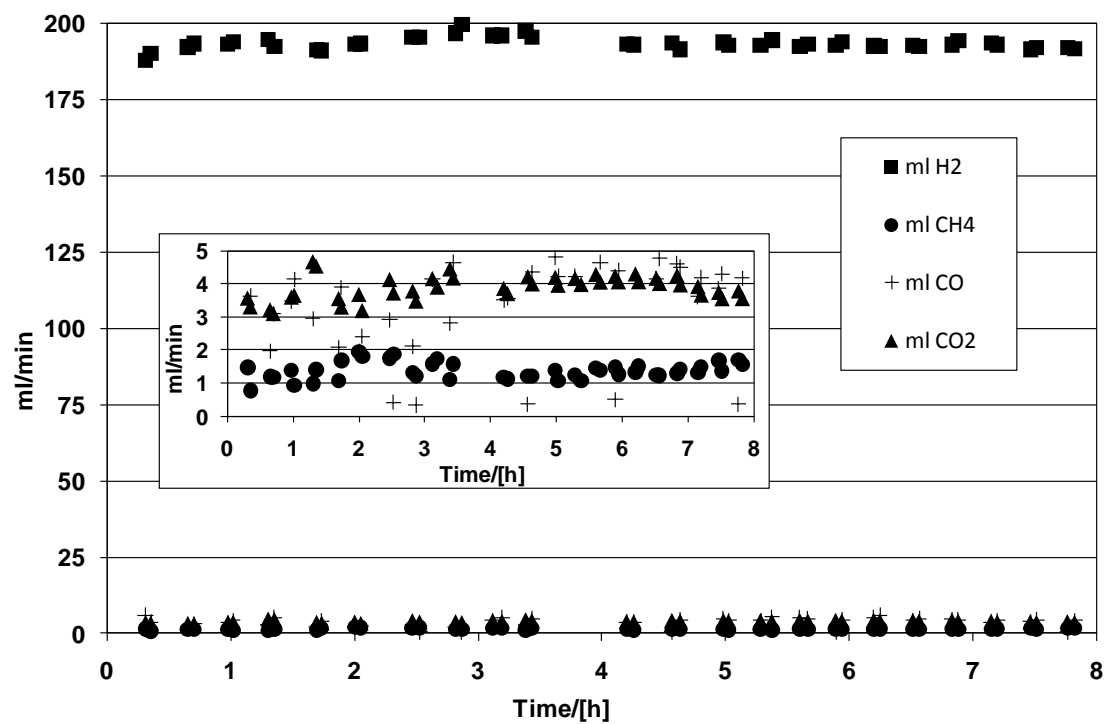


Figure 6

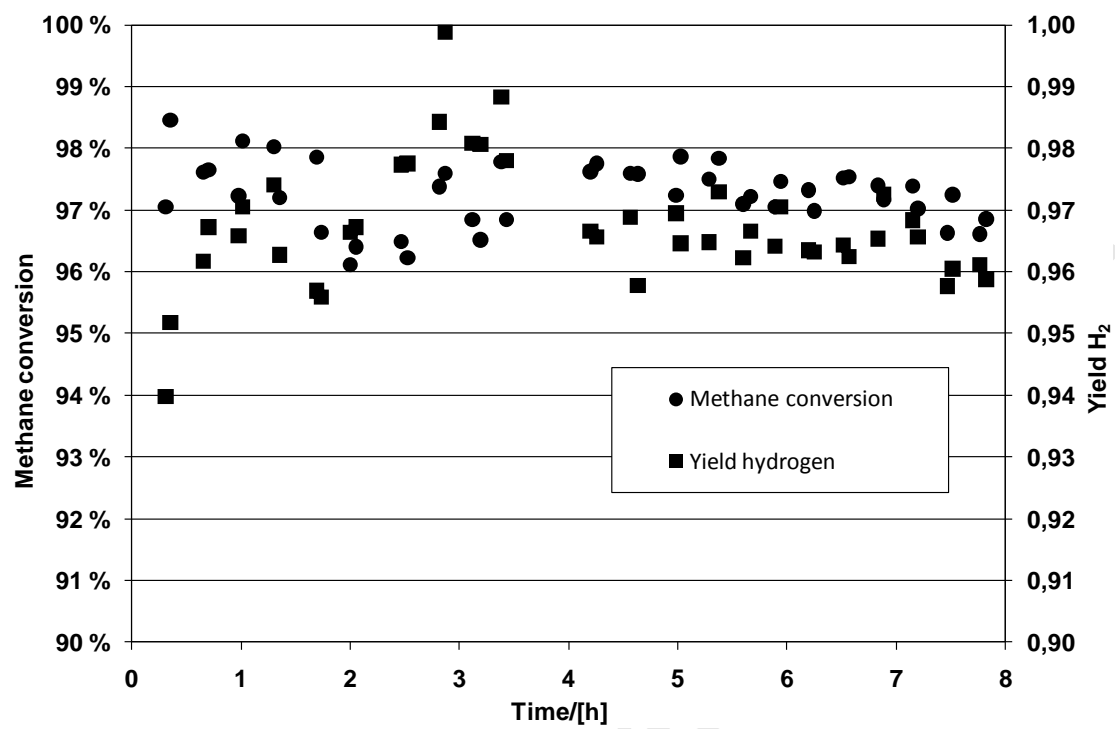
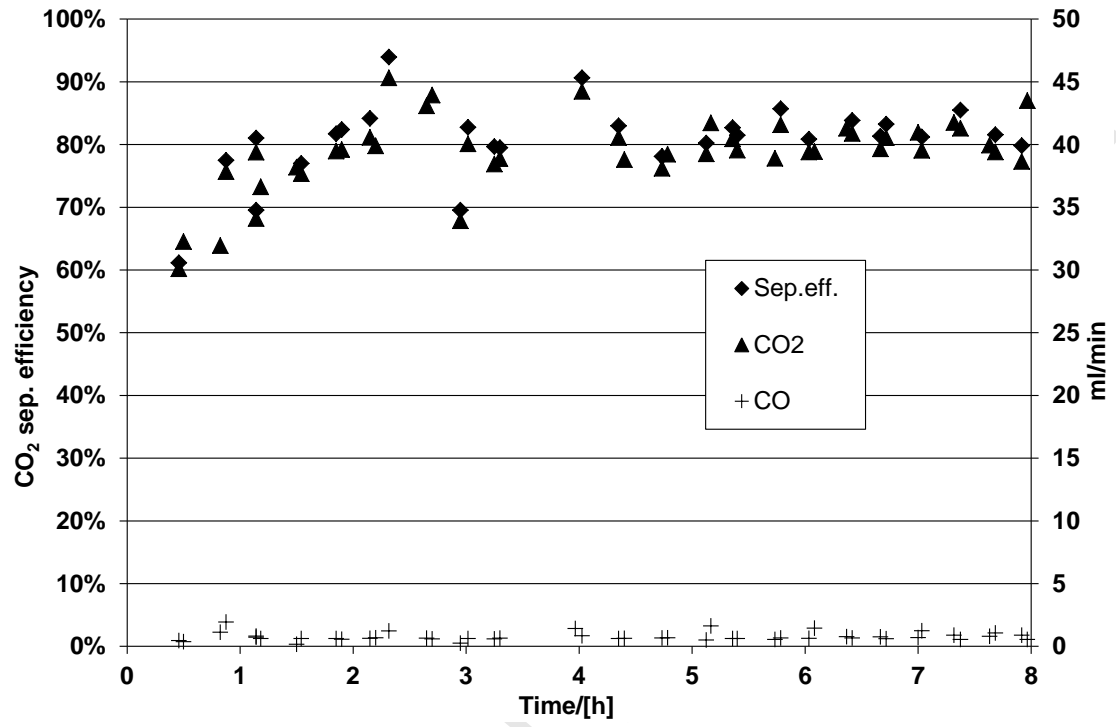


Figure 7



Accepted